DISCRETE PREDATOR-PREY MODEL IN TWO DIMENSIONS

by

Brandon Isensee

Submitted in partial fulfillment of the

requirements for Departmental Honors in

the Department of Mathematics

Texas Christian University

Fort Worth, Texas

May 8, 2023

DISCRETE PREDATOR-PREY MODEL IN TWO DIMENSIONS

Project Approved:

Supervising Professor: Igor Prokhorenkov, Ph.D.

Department of Mathematics

Ken Richardson, Ph.D.

Department of Mathematics

Liran Ma, D.Sc.

Department of Computer Science

ABSTRACT

We show that a discrete two-dimensional logistic predator-prey dynamical system with two parameters undergoes a Neimark-Sacker bifurcation under certain conditions. Our evidence includes numerical computations of eigenvalues, orbits, Lyapunov exponents, and bifurcation diagrams.

Introduction

This paper presents the results of research focused on a discrete predator-prey model in two dimensions. We focus our analysis on a neighborhood of the fixed point with nonzero positive coordinates in the parameter plane. We observe the occurrence of Neimark-Sacker bifurcations alongside other interesting behavior. Section 1 begins with a brief history of dynamics, followed by a discussion of the logistic ordinary differential equation in Section 2. Section 3 delves into the discrete logistic map and the dynamics of its orbits. Section 4 looks at the predator-prey system of differential equations and the long-term behavior of different solutions. Finally, we conclude with our findings from researching the discrete predator-prey model in Section 5.

1 Brief History of Dynamics

The study of dynamical systems was first undertaken by the French mathematician Henri Poincare (1854-1912), who is credited for many important aspects of the field, including the observation of the qualitative behavior of solutions to differential equations; emphasis on the long-term behavior of sets of trajectories; and bifurcations or changes in qualitative behavior dependent on parameters [1, p. 279]. When trying to solve the three-body problem, Poincare also noticed that initial conditions close in value would produce drastically different trajectories of celestial bodies in orbit [4]; this sensitivity to initial conditions is now considered one of the primary characteristics of chaos.

Poincare produced his last geometric insight in 1912, which states that there are infinite periodic solutions for three solar bodies in stable orbits. This conjecture was proved only a year later by the Harvard mathematician George David Birkhoff (1884-1944). In addition, Birkhoff also developed the ergodic theory in his research in ordinary differential equations and their solutions, alongside other contributions to dynamics [2].

In 1960, an American mathematician, Stephen Smale (1930-), discovered the dynamics and chaos associated with a square being transformed into a horseshoe, after receiving a counterexample to a conjecture of his from Norman Levinson (1912-1975). This horseshoe transformation is a geometric interpretation of equations studied by the British mathematicians Mary Cartwright (1900-1998) and J. L. Littlewood (1885-1977) during World War II. He found that the deterministic transformation of the square corresponded with random coin-flipping, making this behavior chaotic [11].

A few years later in 1963, Edward Lorenz (1917-2008) published a paper regarding the discoveries

he made as a meteorologist; it is this publication where the Lorenz equations and Lorenz attractors originate from. He found that for his set of differential equations modeling the atmosphere, the results would be drastically different with slight variations in the initial conditions. This eventually brought him international fame and the importance of chaos became widely recognized, given its application to real-world phenomena [9].

For discrete models, Sharkovsky's theorem, proved in 1964 by the Ukrainian mathematician Oleksandr Sharkovsky (1936-2022), states that the existence of certain cycles implies the existence of other cycles for a one-dimensional continuous map from an interval to itself [10]. In particular, if a map had a 3-cycle, then every possible p-cycle also exists for this map, though these other cycles may not be stable.

In 1975, the American mathematician Mitchell Feigenbaum (1944-2019) discovered what is now called the Feigenbaum constant, 4.6692..., where successive parameter intervals between period-doubling bifurcations shrink by a factor of this constant for unimodal maps, though this result would not be published until 1979. He also created methods for solving ordinary differential equations and interpolation methods [8].

Also in 1975, the word "fractal" entered the vocabulary of mathematics through the Polish mathematician Benoit Mandelbrot (1924-2010). Fractals capture infinitely repeating patterns in a geometric figure, whereby a magnification of a figure's part exhibits similarity to the whole. The Mandelbrot set is one of many mesmerizing fractals and shows the beauty inherent in even simple mathematics. In addition, Mandelbrot also studied "rough" shapes, such as mountains, coastlines, plants, and blood vessels, in an attempt to describe them mathematically [3].

In 1976, Robert May (1936-2020), a biologist at Princeton University at the time, published a paper analyzing the discrete logistic map, written as $x_{n+1} = f(x_n) = k(1 - x_n)x_n$, and investigated its stability, p-cycles, period doubling, and the onset of chaos [7]. This showed mathematicians and scientists that equations simple in appearance can have quite complicated dynamics.

2 Logistic Ordinary Differential Equation

Before our research results are discussed, it may be helpful to understand the dynamics of a one-dimensional differential equation. The logistic differential equation models the dynamics of a population in the presence of limited resources. It is written as

$$\frac{dy}{dt} = k(1 - \frac{y}{N})y,$$

where, in population terms, y is the population and $\frac{dy}{dt}$ gives the population growth rate at time t. $k > 0$ is the growth parameter and N is the carrying capacity. The term $k(1 - \frac{y}{N})$ is the adjusted growth rate, which decreases as y approaches N. The adjusted growth rate becomes negative if $y > N$. The equation's **equilibrium points** are those values of y where $\frac{dy}{dt} = 0$, or when the population stays constant with time. In this case, the equilibrium points are $y = 0$ and $y = N$.

This equation can be non-dimensionalized by setting $y = xN$ and $t = \frac{t'}{k}$, where x and t' are new dimensionless variables. We compute:

$$\begin{aligned}
\frac{d(xN)}{d(\frac{t'}{k})} &= kxN(1 - \frac{xN}{N}), \\
\frac{N}{\frac{1}{k}}\frac{dx}{dt'} &= kxN(1 - x), \\
Nk\frac{dx}{dt'} &= kxN(1 - x), \\
\frac{dx}{dt'} &= x(1 - x).
\end{aligned}$$

The carrying capacity and growth parameter have been scaled to 1, and our equilibrium points are now $x = 0$ and $x = 1$.

2.1 Long-Term Behavior of Solutions for the Logistic Differential Equation

Typical solutions for the non-dimensionalized logistic equation are shown below.

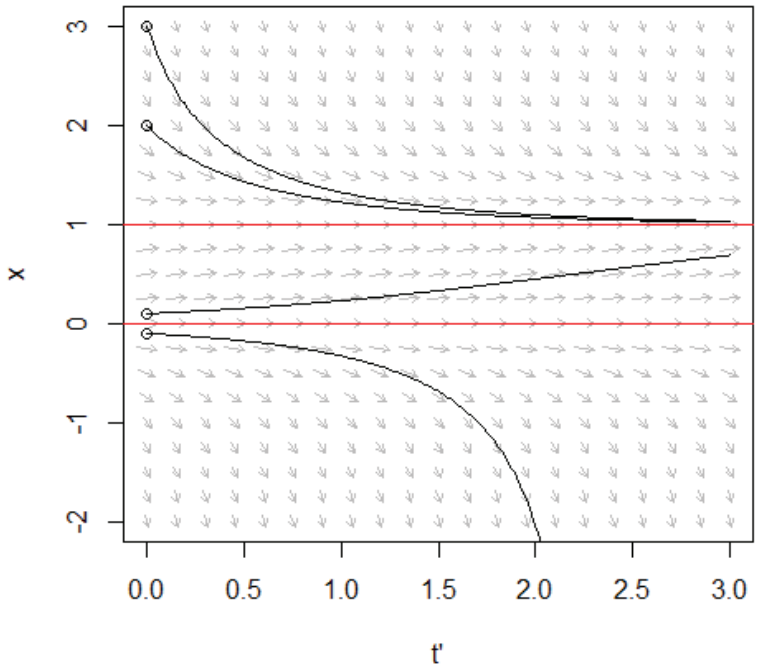

Figure 1: Typical solutions for the logistic equation with different initial conditions.

If $0 < x < 1$, $\frac{dx}{dt'}$ is positive, so the population increases towards $x = 1$. If $x > 1$, $\frac{dx}{dt'}$ is negative, so the population decreases towards $x = 1$. This makes $x = 1$ a stable equilibrium point, since the population moves toward this value, while it moves away from $x = 0$, an unstable equilibrium point. Negative initial conditions will diverge to negative infinity, but they are ignored throughout this paper since a negative population is meaningless.

While we can find a formula for $x(t)$ for the logistic equation through the separation of variables, most differential equations representing one-dimensional dynamical systems will not have formulas for their solutions. In that case, approximate solutions can be obtained by numerical methods. However, we can often obtain information about the long-term behavior of solutions by qualitative methods, which do not require formulas or numerical approximations.

3 Discrete Logistic Map

The discrete logistic map is an analog of the logistic differential equation, where the population is measured at discrete intervals. It is written as

$$x_{n+1} = f(x_n) = k(1 - x_n)x_n,$$

where x_n is the population value at time n and $n = 0, 1, 2, ...$ As before, k represents the growth parameter, and $k_n = k(1 - x_n)$ adjusts the growth rate. If x_n is close to 0, then k_n will be close to k. However, if x_n is close to 1, then k_n will be close to 0 instead. With the logistic ordinary differential equation, we could non-dimensionalize it and scale all the parameters to 1. On the other hand, k in the discrete logistic map cannot be scaled to 1 through non-dimensionalization.

For discrete maps, a sequence of population values $x_0, x_1, x_2, ...x_n, ...$ is called an **orbit**, where x_0 is the orbit's **seed** or **initial condition**.

3.1 Dynamics of Orbits of the Logistic Map

The first step in a study of a discrete dynamical system is the analysis of its fixed points. A point $x = c$ is a **fixed point** if it satisfies $f(c) = c$, such that the population value stays constant for each time step period. For the logistic map, its fixed points are $c = 0$ and $c = 1 - \frac{1}{k}$.

To study the stability of a fixed point $x = c$, we replace the non-linear map $x_{n+1} = f(x_n)$ by its linear approximation near $x = c$: $x_{n+1} = f'(c)x_n$. If $|f'(c)| < 1$, the fixed point is **stable** and attracts nearby orbits. When $|f'(c)| > 1$, $x = c$ is **unstable** and repels nearby orbits. In the marginal case $|f'(c)| = 1$, stability is determined through the higher order terms ignored in linearization. $f'(c)$ for the logistic map is shown below:

$$f'(c) = k(1 - 2c)$$

The stability of $c = 0$ is simply determined by k: the fixed point is stable when $|k| < 1$ and unstable when $|k| > 1$. When we solve $|f'(c)| < 1$ and $|f'(c)| > 1$ for $c = 1 - \frac{1}{k}$, we find it is stable when $1 < k < 3$ and unstable when $k < 1$ or $k > 3$.

Before studying orbits of the logistic map, we restrict k and x_0 such that $k \in [0, 4]$ and $x_0 \in (0, 1)$, so that $x_n \in (0, 1)$ for all n. If $k > 4$, most orbits eventually leave $(0, 1)$ and then diverge to $-\infty$. Qualitatively different behaviors of orbits can be observed for various intervals of k. For instance, when $0 < k \leq 1$, the population is always driven to extinction. This aligns with the stability conditions for $c = 0$ as shown above. By contrast, the population will stabilize towards $c = 1 - \frac{1}{k}$ when $1 < k \leq 3$. Various orbits are shown below together with their respective values of the parameter k and initial conditions x_0.

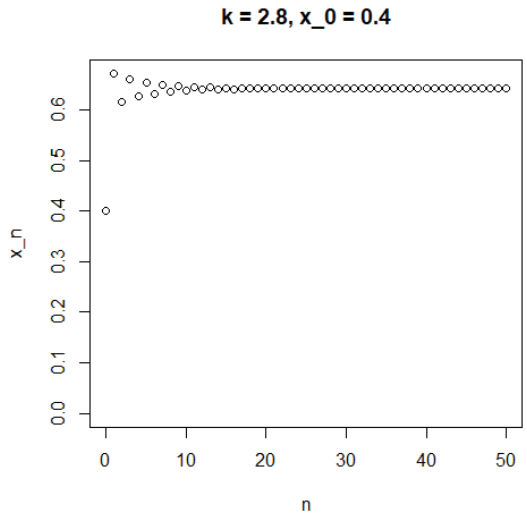

(a) The population stabilizes towards the fixed point $c \approx 0.643$.

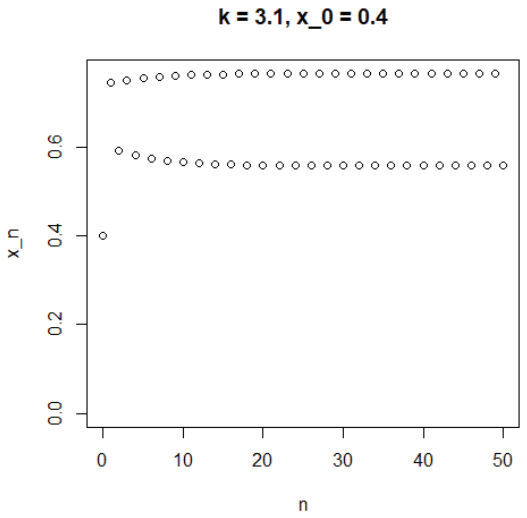

(b) When $k = 3.1$, the population stabilizes towards a 2-cycle, since $c = 1 - \frac{1}{k}$ is now unstable.

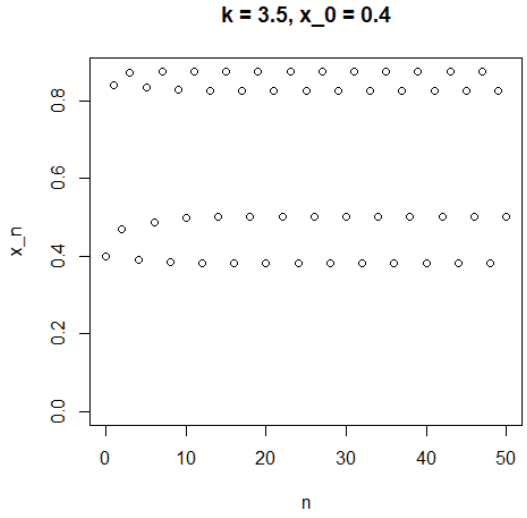

(c) The population stabilizes towards a 4-cycle, since the 2-cycle is unstable when $k = 3.5$.

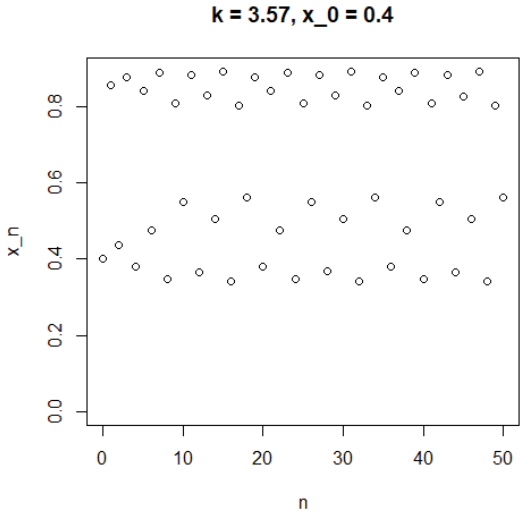

(d) A stable 8-cycle appears. Period-doubling continues as k increases.

Figure 2: The long-term behavior of an orbit changes depending on the value of k.

When $k > 3$, $c = 1 - \frac{1}{k}$ becomes unstable. For $3 < k < 1 + \sqrt{6}$, numerical experiments show a 2-cycle forming near $c = 1 - \frac{1}{k}$. Now, orbits oscillate between two different values near the fixed point. Orbits undergo **period-doubling** as k increases: the 2-cycle becomes unstable as a stable 4-cycle is born, which then turns unstable as a stable 8-cycle is born, and so forth.

In mathematical notation, a 2-cycle exists for a map $x_{n+1} = f(x_n)$ when there is a value x such that $f(f(x)) = x$, or $f^2(x) = x$, where x is not a fixed point. The equation for a p-cycle is $f^p(x) = x$.

As k increases from 3 to approximately 3.56995, the period-doubling occurs faster and faster. Specifically, the k intervals where these p-cycles exist shrink by the Feigenbaum constant 4.669, a feature that is characteristic of all unimodal maps [12, p. 379-380]. We can make a bifurcation diagram by plotting the long-term behavior of the orbits of the logistic map for different k values along an interval. We use these diagrams to illustrate where bifurcations occur, which are defined as qualitative changes in behavior of orbits to the map.

To create the graphs below, 800 equally spaced values of k on $0 \leq k \leq 4$ and $3.3 \leq k \leq 4$ are calculated in a program in R. For each k value, a random seed $x_0 \in (0, 1)$ is chosen and its orbit $x_0, x_1, ..., x_{800}$ is calculated. Only $x_{501}, ..., x_{800}$ are plotted for the k value, which removes any transient behavior. The diagrams are shown below. It should be noted that for almost any choice of seed such that $0 < x_0 < 1$, the long-term behavior of the orbit will be the same.

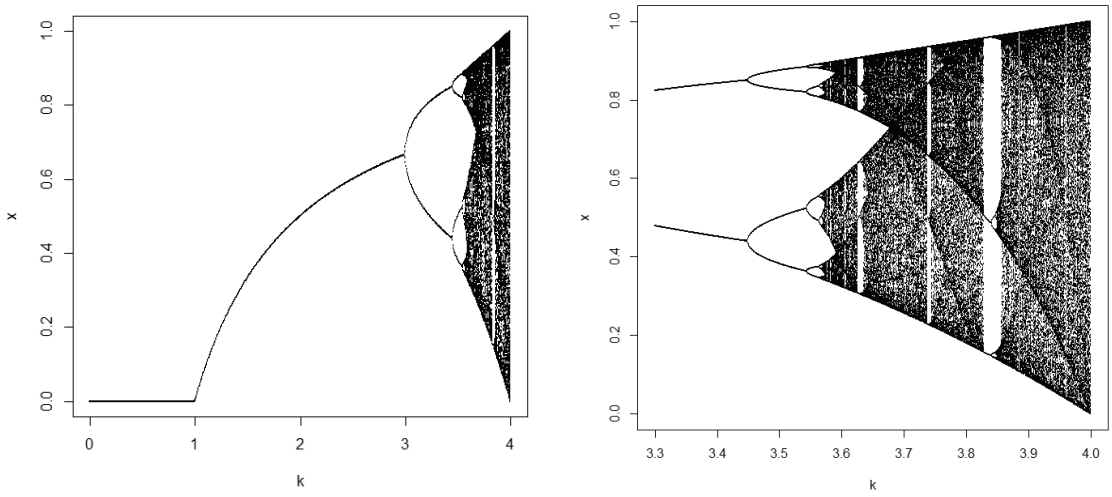

Figure 3: Bifurcation diagrams for the logistic map. The right graph is magnified on $k \in [3.3, 4]$.

When $0 < k < 1$, the population is driven to extinction. For k values between 1 and 3, the population eventually stabilizes toward the fixed point $c = 1 - \frac{1}{k}$; note that we see this same behavior in Figure 2 when $k = 2.8$. On the diagram, this translates to one "branch." As mentioned before, we see the stable 2-cycle appearing at $k = 3$, where the single branch splits into the two values the population will oscillate between. Again, this matches up with the graph in Figure 2 when $k = 3.1$. At $k = 1 + \sqrt{6}$, the 2-cycle becomes unstable and a stable 4-cycle is born, resulting in the two branches splitting into four.

As for bifurcations themselves, one occurs at $k = 1$, since $c = 0$ becomes unstable and $c = 1 - \frac{1}{k}$ becomes stable. A **pitchfork bifurcation** occurs at $k = 3$, since a 2-cycle is born when $c = 1 - \frac{1}{k}$ becomes unstable.

3.2 Chaotic Behavior of Orbits

Period-doublings occur faster and faster, until $k \approx 3.56995$ where periodic orbits of period 2^n are all unstable. For certain values beyond $k \approx 3.56995$, orbits behave chaotically. In this state, orbits no longer stabilize towards fixed points. Furthermore, initial conditions close in value will have significantly different orbits over time.

However, chaos is not random. That is, a seed completely determines the resulting orbit. The logistic map is deterministic, so an initial condition for a given k will always have the same orbit [12, p. 331]. We are also more interested in orbits that stay bounded. For orbits that diverge, $\pm\infty$ acts as a fixed point, which makes these orbits not aperiodic [12, p. 331]. Putting all of the above together, **chaos** is defined as the state where orbits are aperiodic, deterministic, and exhibit sensitivity to initial conditions.

It is also important to note that, although it may appear so in Figure 3, there are no intervals of chaos. In fact, for any interval of k values, one can find periodic orbits inside the interval [6].

What indicators are there for chaos? One common way a dynamical system approaches chaos is through a sequence of 2^n-cycles, as can be observed in the bifurcation diagrams in Figure 3. Another indicator is when the Lyapunov exponent for the system is positive, whose calculation is discussed in the next section.

3.3 Lyapunov Exponent

We can also calculate the Lyapunov exponent for the logistic map, which informs us how quickly nearby trajectories converge or diverge. The distance between two points on two different trajectories at time n is approximated by the relation $|d(n)| \approx |d(0)|e^{\lambda t}$ or by $|d(n)| \approx |d(n-1)|e^{\lambda}$, where λ is the Lyapunov exponent [12, p. 373]. We can rearrange the equations to solve for λ:

$$\lambda \approx \frac{\ln\left(|d(n)|/|d(0)|\right)}{n}$$

Positive values indicate exponential divergence of nearby trajectories, while negative values imply

exponential convergence. The more positive or negative the Lyapunov exponent is, the faster trajectories diverge or converge. Estimates for the exponent are shown below for k values on the interval [0,1].

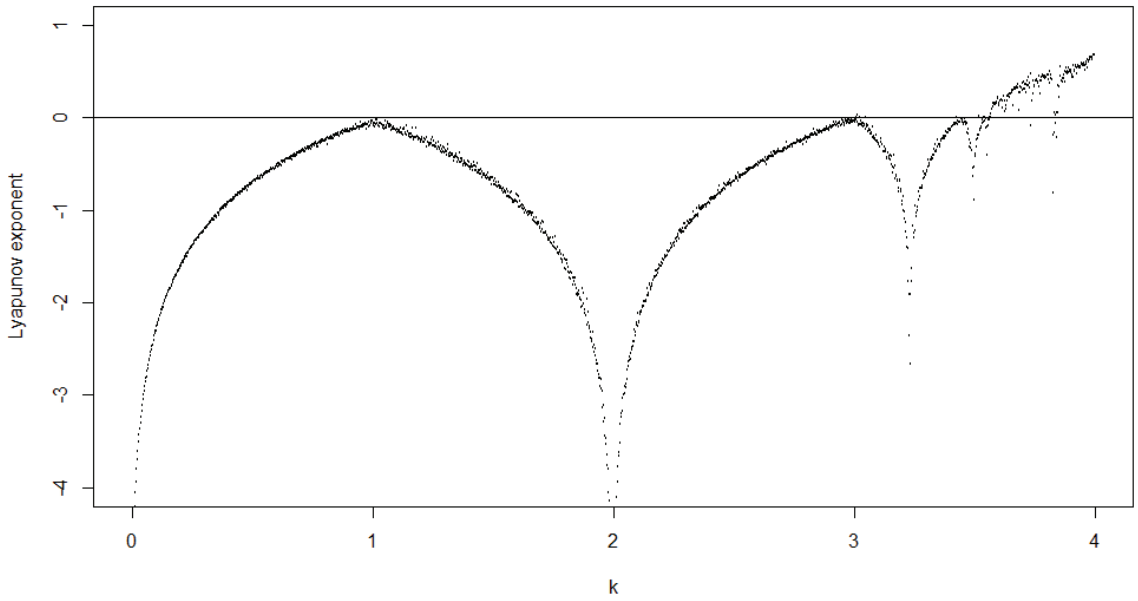

Figure 4: Graph of the Lyapunov exponent

The Lyapunov exponent estimates can be used to predict bifurcation values via changes in stability of the fixed points or p-cycles. The local maximums or "peaks" of the graph coincide with those k values where bifurcations occur. For instance, the flip bifurcation at $k = 1$ and the pitchfork bifurcation at $k = 3$ in Figure 3 coincide with local maximums in Figure 4. For some values of k, the Lyapunov exponent reaches $-\infty$, making the fixed point or p-cycle superstable, whereby the orbits stabilize rapidly.

The Lyapunov estimates throughout this paper are calculated in R. For the logistic map, $\lambda = \lim_{n\to\infty} \sum_{i=0}^{n} \frac{\ln|k-2kx_i|}{n}$ [12, p. 373], though $n = 100$ when estimating in R. To see the raw code which contains the method for estimating Lyapunov estimates for the discrete predator-prey system, see Appendix A.

4 Predator-Prey System of Differential Equations

Before our study of the two dimensional discrete predator-prey system, we briefly describe the continuous case. The system is as follows:

$$\frac{dx}{dt} = k_1(1-x)x + axy$$
$$\frac{dy}{dt} = k_2(1-y)y - bxy,$$

where x is the predator population and y is the prey population, and the parameters k_1, k_2, a, and b are all greater than 0. In addition to the logistic terms, each equation also has an interaction term, axy and bxy. In the absence of one population, the equation for the other population reduces to a logistic ordinary differential equation. The variables k_1 and k_2 are the growth rate parameters for the populations, while a and b determine how the predator and prey populations interact. When there is a bigger y population, the predator population benefits and has a larger growth rate. Conversely, when there is a larger x population, the prey population suffers a lower population growth rate. For simplification, we set a and b equal to 1.

An equilibrium point (x_p, y_p) exists when $\frac{dx}{dt} = 0$ and $\frac{dy}{dt} = 0$. For this system, these points are $(0,0)$, $(1,0)$, $(0,1)$, and $(\frac{k_1k_2+k_2}{k_1k_2+1}, \frac{k_1k_2-k_1}{k_1k_2+1})$.

4.1 Stability of Equilibrium Points

In two dimensions, an equilibrium point's stability is determined by the eigenvalues of the Jacobian matrix computed at the equilibrium point; this matrix gives the linear approximation to the system at an equilibrium point. To find the eigenvalues, we first find the Jacobian matrix

$$J_f = \begin{bmatrix} k_1 - 2k_1x_p + y_p & x_p \\ -y_p & k_2 - 2k_2y_p - x_p \end{bmatrix},$$

where x_p and y_p are the coordinates of a fixed point for the system. We then take the determinant of the matrix $J_f - \lambda I$ and solve for the eigenvalues $\lambda_{1,2}$. Since $(\frac{k_1k_2+k_2}{k_1k_2+1}, \frac{k_1k_2-k_1}{k_1k_2+1})$ is the only fixed point whose coordinates depend on the growth rate parameters, we solve $\lambda_{1,2}$ for this point in terms of k_1 and k_2, which produces the following:

$$\lambda_{1,2} = \frac{q \pm \sqrt{q^2 - 4r}}{2}, \text{where}$$
$$q = k_1 - 2k_1x_d + y_d + k_2 - 2k_2y_d - x_d,$$
$$r = (k_1 - 2k_1x_d + y_d)(k_2 - 2k_2y_d - x_d) + x_dy_d,$$
$$x_d = \frac{k_1k_2 + k_2}{k_1k_2 + 1},$$
$$y_d = \frac{k_1k_2 - k_1}{k_1k_2 + 1}$$

For a two-dimensional system of ordinary differential equations, an equilibrium point is stable if both eigenvalues are negative, or unstable if at least one eigenvalue is positive. If $\lambda_1 < 0 < \lambda_2$, the point is a saddle, where nearby trajectories may initially be attracted to the fixed point before diverging. When both eigenvalues equal 0, this is a marginal case and the equilibrium point's stability must be determined through other means. If the eigenvalues are complex such that $\lambda_{1,2} = \alpha + \beta i$, the point is unstable when $\alpha < 0$ and stable when $\alpha > 0$. If $\alpha = 0$, nearby trajectories can form a closed orbit around the equilibrium point, though its existence and stability depend on higher order terms in the approximation.

Graphs below show which parameter regions produce a stable or unstable fourth equilibrium point with real or complex eigenvalues. For the graph on the left, colored regions indicate parameter values associated with real eigenvalues for $(\frac{k_1k_2+k_2}{k_1k_2+1}, \frac{k_1k_2-k_1}{k_1k_2+1})$, where red is stable, blue is unstable, and purple are saddle nodes. The gray regions on the right graph indicate parameter values associated with complex eigenvalues, where dark gray is stable and light gray is unstable. Values on the line $k_2 = -k_1$ for $k_1 \in (-1, 1)$ cause $\alpha = 0$, which may lead to closed orbits around the fourth equilibrium point.

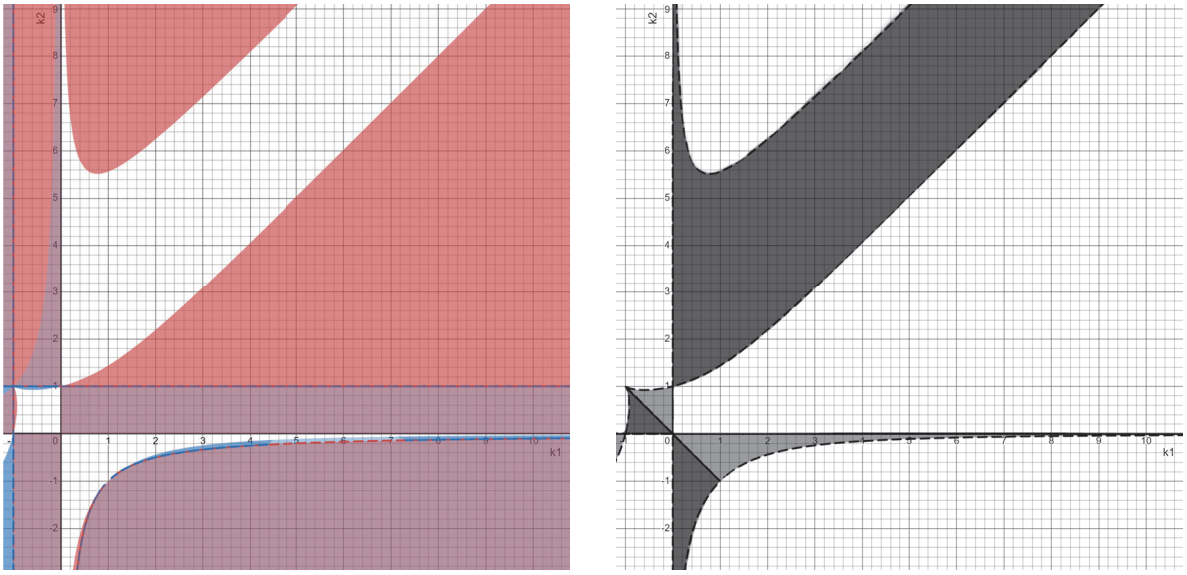

Figure 5: Real and complex graphs showing the stability regions for $(\frac{k_1k_2+k_2}{k_1k_2+1}, \frac{k_1k_2-k_1}{k_1k_2+1})$.

4.2 Long-Term Behavior of Solution Curves

Phase portraits of the predator-prey system are given below for varying values of k_1 and k_2, along with trajectories with their initial conditions. Equilibrium points are plotted in red.

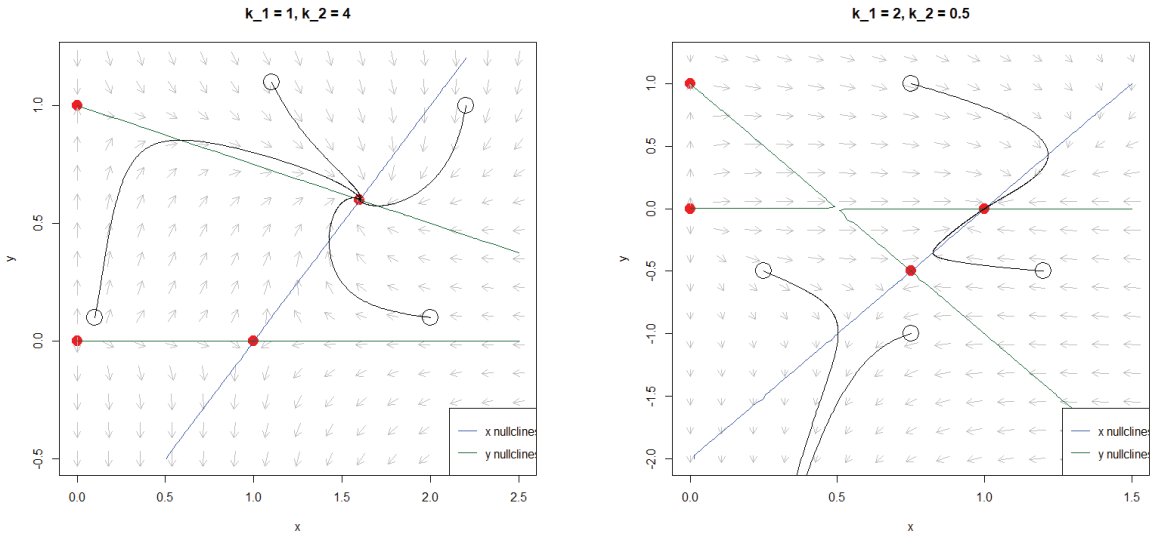

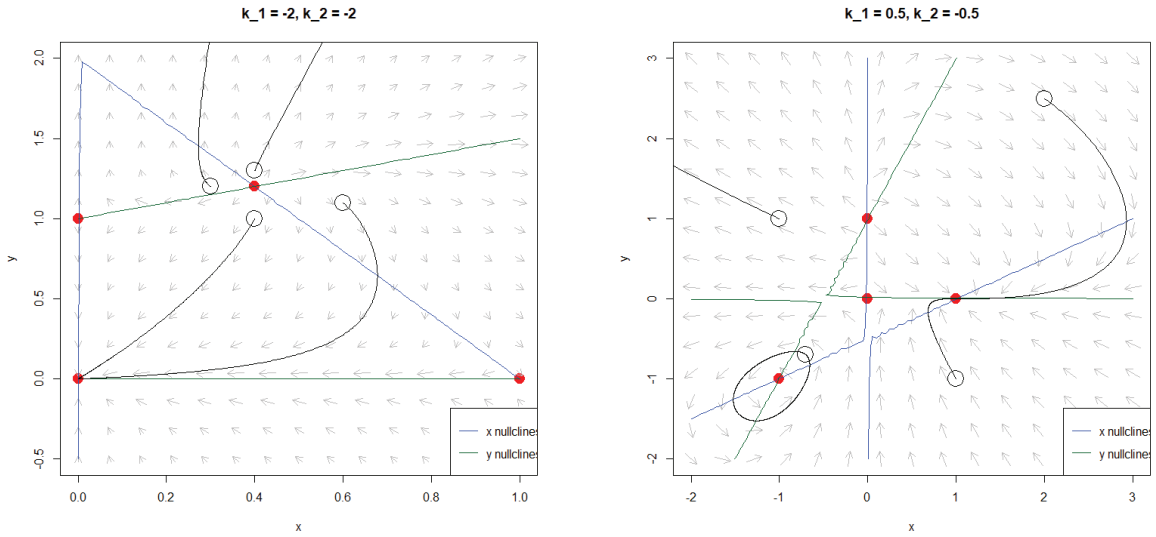

Figure 6: The long-term behavior of the solution curves depends on which growth parameter values and initial conditions are chosen.

In the first phase portrait, most trajectories converge to the fourth equilibrium point. Since the first portrait has complex eigenvalues for its fourth equilibrium point, it is called a spiral sink. In biological terms, both populations are able to coexist without driving the other to extinction. For the second phase portrait, the eigenvalues satisfy $\lambda_1 < 0 < \lambda_2$, so the fourth equilibrium point is a saddle node. Nearby trajectories are attracted to it before diverging either towards $-\infty$ or to a nearby stable equilibrium point.

The fourth equilibrium point in the third graph has complex eigenvalues such that $|\lambda_{1,2}| > 1$, so nearby trajectories spiral away from the point. As such, this equilibrium point is called a spiral source. Both populations may grow indefinitely or be driven to extinction depending on initial conditions. Finally, the fourth graph confirms that solutions can form closed orbits around the fourth equilibrium point.

It is important to mention that while some trajectories may stabilize towards an equilibrium point in the long run, they will never actually reach it. Otherwise, all nearby trajectories would intersect at the equilibrium point, violating the existence and uniqueness theorem [12, p. 150].

Note that for certain values of k_1 and k_2, the fourth equilibrium point can have negative coordinates. Since negative populations are impossible, we ignore equilibrium points and initial conditions with negative coordinates. For the next section, we will focus our study on parameter values that produce a fourth equilibrium point with positive nonzero coordinates.

5 Discrete Predator-Prey System

Our research focuses on a discrete predator-prey system, which is an analog of the continuous predator-prey system. It is written as

$$x_{n+1} = f(x_n, y_n) = k_1(1 - x_n)x_n + ax_ny_n$$
$$y_{n+1} = g(x_n, y_n) = k_2(1 - y_n)y_n - bx_ny_n,$$

where k_1, k_2, a, and b are greater than 0. These equations have the same terms and parameters as in the continuous case, but are now modeled in discrete, rather than continuous, time. As a result, this system can exhibit very different behavior from its continuous counterpart. As before, we set $a = b = 1$.

5.1 Stability of Fixed Points

As before, our first step in studying the dynamics of orbits to this system is to calculate its fixed points and study their stability. A fixed point (c, d) exists when $f(c, d) = c$ and $g(c, d) = d$. For this system, these points are $(0, 0)$, $(\frac{k_1-1}{k_1}, 0)$, $(0, \frac{k_2-1}{k_2})$, and $(\frac{k_1k_2-1}{k_1k_2+1}, 1 - \frac{2k_1}{k_1k_2+1})$. Calculating the eigenvalues to determine stability follows the same process as in Section 4.1. However, the conditions for stability are different between discrete and continuous systems. The fixed point is stable when $\max\{|\lambda_1|, |\lambda_2|\} < 1$, and unstable when one or both eigenvalues have magnitudes greater than 1.

If $\lambda_{1,2} = \alpha \pm \beta i$, then the point is stable when $|\lambda_{1,2}| < 1$ and unstable when $|\lambda_{1,2}| > 1$. Since the fourth fixed point $(\frac{k_1k_2-1}{k_1k_2+1}, 1 - \frac{2k_1}{k_1k_2+1})$ is the only one that can have positive real coordinates, our research focuses on the behavior of the orbits near this point. We first solve for the eigenvalues of the Jacobian matrix computed at the fourth fixed point to determine its stability:

$$\lambda_{1,2} = \frac{q \pm \sqrt{k_1^2k_2^4 + rk_2^3 + sk_2^2 + tk_2 + u}}{2(k_1k_2 + 1)}, \text{where}$$
$$q = -k_1^2k_2 - k_1k_2^2 + k_1 - k_2 + 4k_1k_2 + 2,$$
$$r = -2k_1^3 - 4k_1^2 + 2k_1,$$
$$s = k_1^4 + 4k_1^3 - 4k_1 + 1,$$
$$t = -2k_1^3 + 4k_1^2 + 2k_1,$$
$$u = k_1^2 - 8k_1 + 4$$

Before graphing the parameter regions, we require that $\frac{k_1k_2-1}{k_1k_2+1} > 0$ and $1 - \frac{2k_1}{k_1k_2+1} > 0$. If either

the predator or prey population equals zero, the system of equations reduces to a logistic map, whose behavior we already studied. With these restrictions, we produce the graph below.

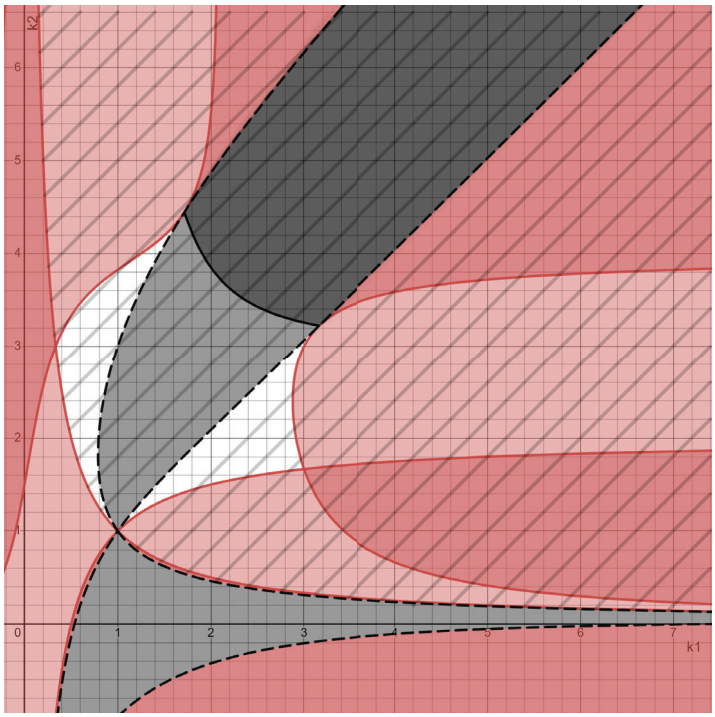

Figure 7: Real and complex areas showing the stability regions for $(\frac{k_1k_2-1}{k_1k_2+1}, 1-\frac{2k_1}{k_1k_2+1})$.

Red regions indicate parameter values associated with an unstable fixed point with real eigenvalues (light red means saddle, though orbits ultimately diverge from it), while the white areas are stable with real eigenvalues. The gray areas indicate complex eigenvalues; the light regions are stable, while the dark region is unstable. The hatched area is where $(\frac{k_1k_2-1}{k_1k_2+1}, 1-\frac{2k_1}{k_1k_2+1})$ has positive coordinates.

5.2 Dynamics of Orbits for the Discrete Predator-Prey System

For a pair of complex eigenvalues, $\lambda_{1,2} = \alpha \pm \beta i$, a **Neimark-Sacker bifurcation** occurs for k_1 and k_2 values where $|\lambda_{1,2}| = 1$ [5]. After the bifurcation, the fixed point changes stability and a closed invariant curve forms around it. These bifurcations can be either supercritical or subcritical. In the **supercritical** case, the invariant curve is stable and the fixed point inside is unstable. The reverse is true for a **subcritical** Neimark-Sacker bifurcation: the invariant curve is unstable while the interior fixed point is stable. The solid black border separating the two complex regions in Figure 8 consist of those parameter values associated with this bifurcation.

Bifurcation diagrams for x_n and y_n when $k_2 = 3.5$ as k_1 varies are shown below together with their Lyapunov exponents over the same intervals. Numerical computations show a supercritical Neimark-

Sacker bifurcation at $k_1 \approx 2.3705$, producing a funnel-like shape that continues to expand. This funnel shape is the stable invariant curve that forms around the fixed point $(\frac{k_1k_2-1}{k_1k_2+1}, 1 - \frac{2k_1}{k_1k_2+1})$.

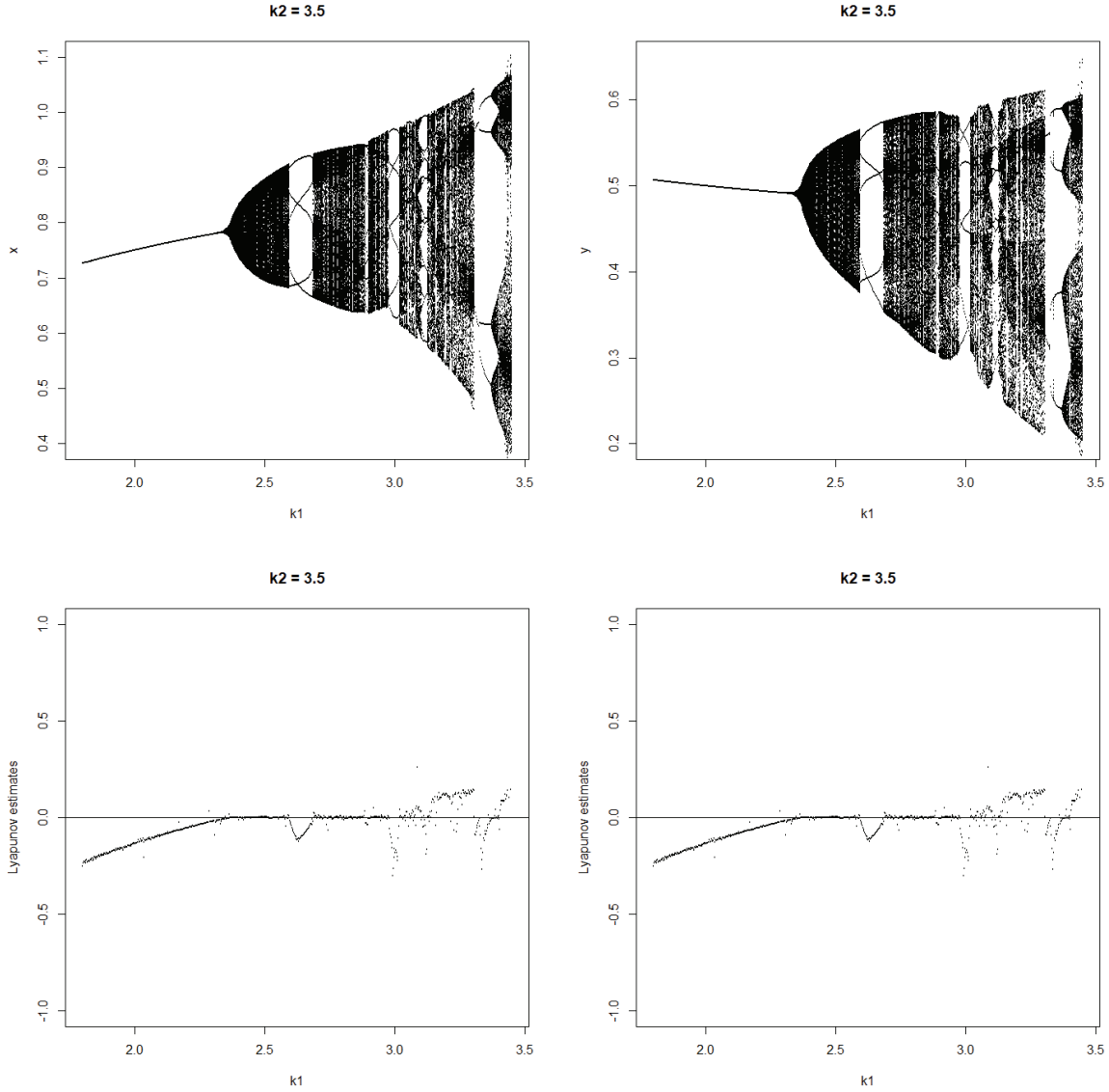

Figure 9: Bifurcation diagrams and Lyapunov exponent estimates.

For certain intervals of k_1, the curve disintegrates and a p-cycle takes its place, though not all of these cycles undergo period-doubling. A 5-cycle exists between $k_1 \approx 2.59918$ and $k_1 \approx 2.67974$, but no other $5 \cdot 2^n$-cycle is observed immediately afterward. It may look like the 5-cycle becomes a 3-cycle for the x_n bifurcation diagram, but that is only because two of the points in the cycle share similar x coordinates. Their y_n coordinates will be different; see Figure 10 when $k_1 = 2.628$. There is also a 12-cycle, a 7-cycle, a 16-cycle, and a 9-cycle, some of which undergo period-doubling when k_1 decreases.

Graphs of x_n and y_n with different k_1 values are given below to illustrate the long-term behavior associated with these parameter values as shown in the bifurcation diagrams in Figure 9. These graphs are created by calculating $(x_0, y_0), ..., (x_{1001}, y_{1001})$, then plotting only $(x_{300}, y_{300}), ..., (x_{1001}, y_{1001})$.

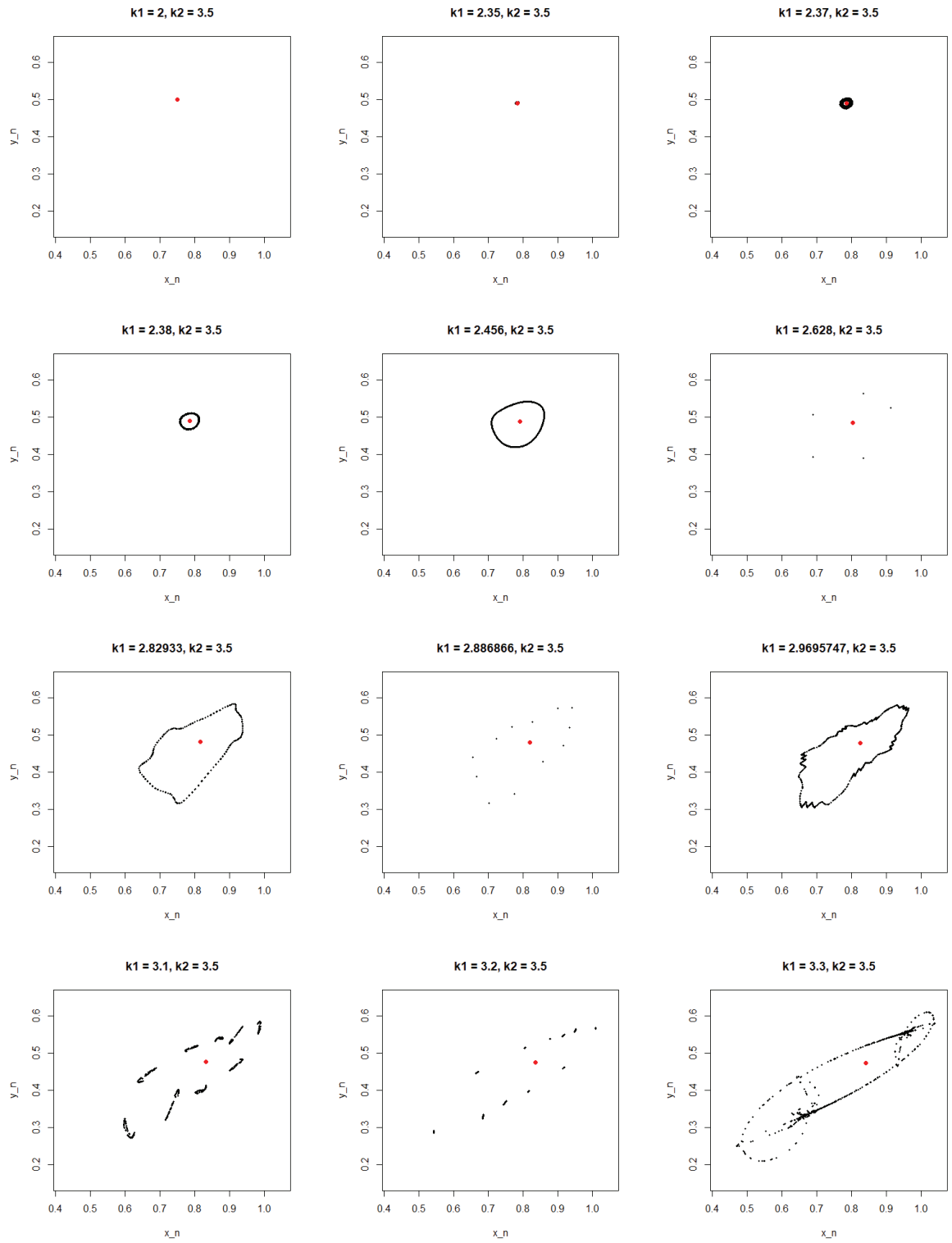

Figure 10: The long-term behavior of the orbits significantly changes depending on the k_1 value chosen.

As k_1 approaches approximately 2.3705 where the Neimark-Sacker bifurcation occurs, the orbit spirals much more slowly towards the fixed point. We first see the invariant curve when $k_1 = 2.38$ in Figure 10. As k_1 increases, we see some of the p-cycles from the bifurcation diagrams appear, such as the 5-cycle when $k_1 = 2.628$ and the 12-cycle when $k_1 = 2.886866$. When there isn't an p-cycle, the shape and number of points on the curve can vary drastically with just slight variations in k_1.

For Figures 9 and 10, the initial condition is close enough to the fixed point that it stabilizes towards it, then the invariant curve after it is born. However, this fixed point is not globally stable for all k_1. At $k_1 \approx 2.133306$, a stable 3-cycle near $(\frac{k_1k_2-1}{k_1k_2+1}, 1 - \frac{2k_1}{k_1k_2+1})$ is born, which undergoes period doubling as k_1 increases. Eventually, three open curves form around the fixed point. Presumably, these curves become unstable, as orbits only stabilize towards the invariant curve after $k_1 \approx 2.414915$. Graphs of x_n and y_n illustrating this behavior are shown below.

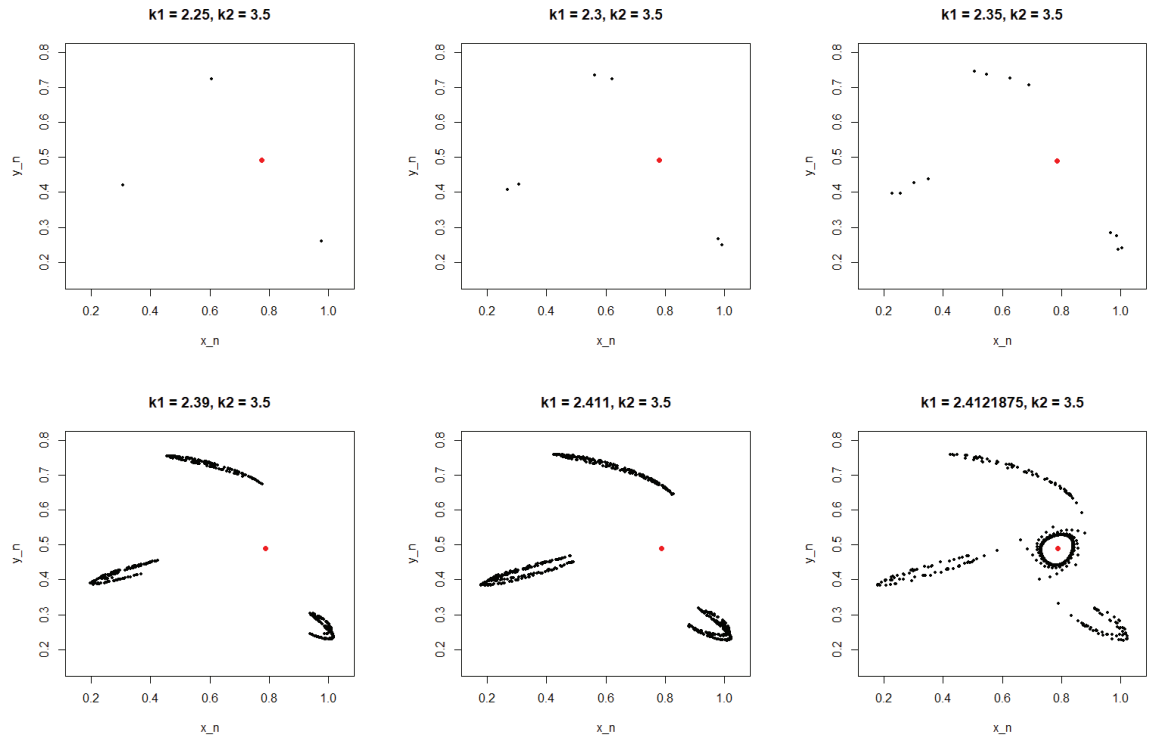

Figure 11: (x_0, y_0) is close to one of the fixed points in the nearby $3 \cdot 2^n$-cycle, causing it to stabilize to the cycle rather than $(\frac{k_1k_2-1}{k_1k_2+1}, 1 - \frac{2k_1}{k_1k_2+1})$ before the Neimark-Sacker bifurcation occurs.

Orbits that stabilize towards the $3 \cdot 2^n$-cycle/open curves also change the Lyapunov exponent estimates along the same interval of k_1. Bifurcation diagrams and their Lyapunov exponents are shown below for comparison.

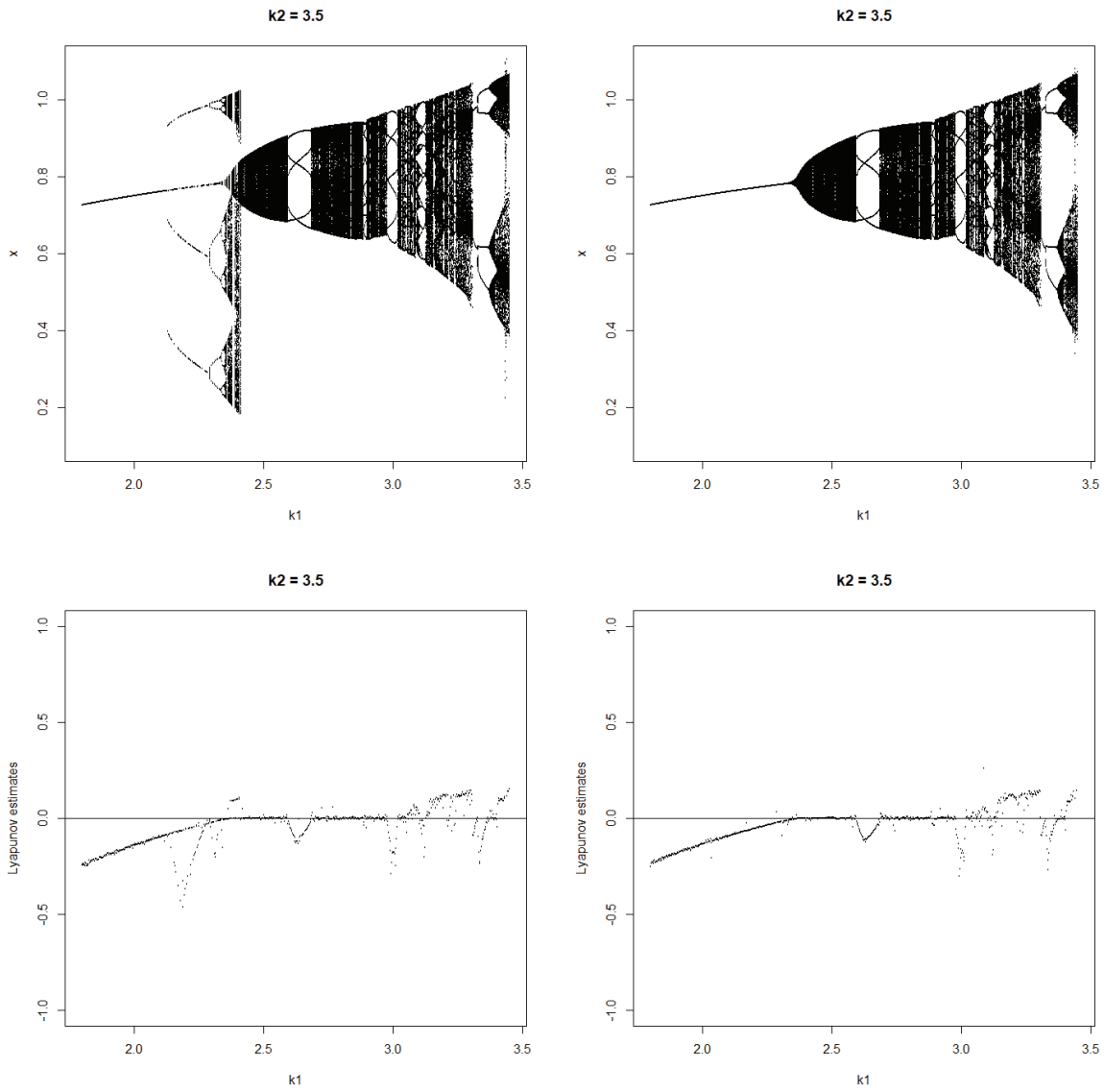

Figure 13: Bifurcation diagrams and Lyapunov exponent estimates for different initial conditions.

In addition to these graphs, videos may be viewed online showing the long-term behavior changing when $k_2 = 3.5$ as k_1 varies. One is a "k-lapse," where every frame shows a graph for each k_1 value on the interval $[2.3, 3.45]$. The other shows the same phenomenon, but is plotted in three dimensions, allowing the viewer to better visualize the bifurcation diagrams in Figure 10. The links to these videos, as well as the code for creating 2- and 3-dimensional bifurcation diagrams for any interval of k_1 or k_2, may be found in Appendix A.

Another phenomenon similar to the Neimark-Sacker bifurcation occurs. At certain values of k_1 and k_2, the curve devolves into either a 2-cycle or a 4-cycle. As the varied growth parameter increases, various invariant curves form around the p-cycle's fixed points. It is unknown under what conditions

these invariant curves form, as they appear when the eigenvalues for the Jacobian matrix at $(\frac{k_1k_2-1}{k_1k_2+1}, 1-\frac{2k_1}{k_1k_2+1})$ are either real or complex. Graphs showing these bifurcations occurring are given below.

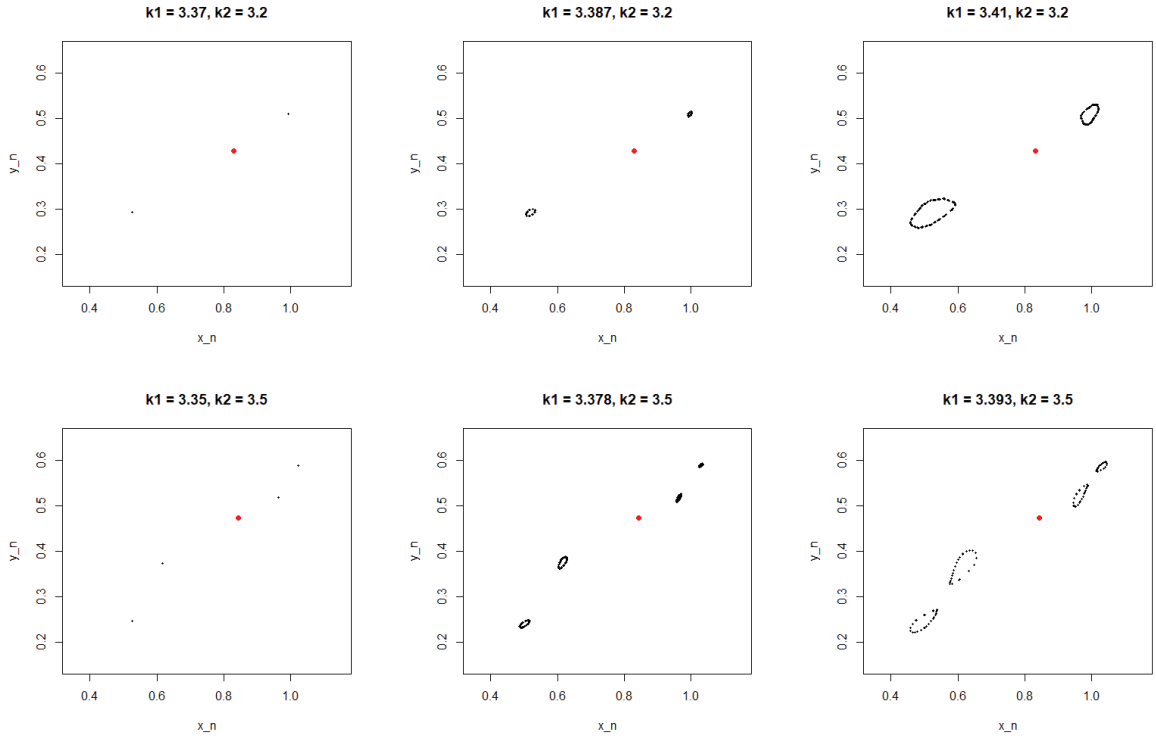

Figure 14: The eigenvalues for the Jacobian matrix at the fourth fixed point are real when $k_2 = 3.2$, but are complex when $k_2 = 3.5$.

5.3 Comparisons Between One- and Two-Dimensional Dynamics

The dynamics of orbits can be quite different between the discrete logistic map and the discrete predator-prey system. For one, the choice of seed when $0 < x_0 < 1$ for the logistic map did not affect the long-term behavior of the orbit. However, seeds that are far enough from the fourth fixed point in the predator-prey system may stabilize to a $3 \cdot 2^n$-cycle before a Neimark-Sacker bifurcation occurs. Another difference is the occurrence of more interesting behavior. The aforementioned Neimark-Sacker bifurcation cannot occur in one-dimensional maps. Chaotic behavior may also more clearly form two-dimensional patterns, called strange attractors, as shown in Figure 15. Strange attractors consist of fractal sets where orbits are aperiodic and are sensitive to initial conditions [12, p. 333]. While the orbit in Figure 15 is aperiodic, the points form a rather curious curve around the fixed point.

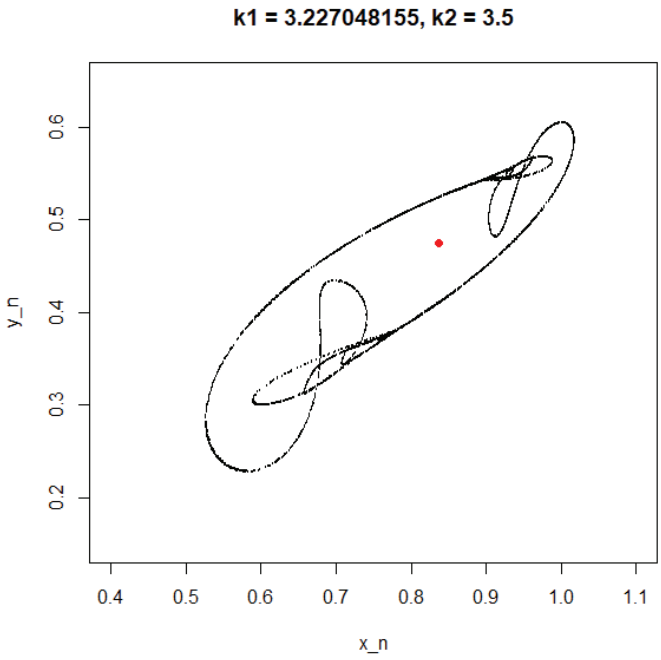

Figure 15: Strange attractor around the fourth fixed point.

5.4 Future Directions

The results discussed in the previous sections raise interesting questions for further inquiry. Many interesting curves form around the fixed point for certain k_1 values, such as that in Figure 15. What are the fractal dimensions of these curves? Another question to study regards the basins of attractions of the fixed points and invariant curves, especially for those parameter values where orbits stabilize either to the fixed point $(\frac{k_1k_2-1}{k_1k_2+1}, 1-\frac{2k_1}{k_1k_2+1})$ or the $3 \cdot 2^n$-cycle.

References

[1] David Aubin and Amy Dahan Dalmedico. Writing the History of Dynamical Systems and Chaos: Longue Durée and Revolution, Disciplines and Cultures. *Historia Mathematica*, 29(3):273–339, Aug 2002.

[2] The Editors of Encyclopaedia Britannica. George David Birkhoff. https://www.britannica.com/biography/George-David-Birkhoff, Mar 2023.

[3] New World Encyclopedia contributors. Benoit mandelbrot, 2022.

[4] Jeremy John Gray. Henri Poincaré. https://www.britannica.com/biography/Henri-Poincare, 2022.

[5] Y. A. Kuznetsov and R. J. Sacker. Neimark-Sacker bifurcation. *Scholarpedia*, 3(5):1845, 2008. revision #91556.

[6] Mikhail Lyubich. The quadratic family as a qualitatively solvable model of chaos. *Notices of the American Mathematical Society*, 47(9):1042–1052, 2000.

[7] Robert M. May. Simple mathematical models with very complicated dynamics. *Nature*, 261(5560):459–467, 1976.

[8] J. J. O'Conner and E. F. Robertson. Mitchell feigenbaum - biography, Sep 2009.

[9] J. J. O'Connor and E. F. Robertson. Edward Norton Lorenz. https://mathshistory.st-andrews.ac.uk/Biographies/Lorenz_Edward/, Jul 2008.

[10] A. Nikolayevich Sharkovsky. Sharkovsky ordering. *Scholarpedia*, 3(5):1680, 2008. revision #91762.

[11] Steve Smale. Finding a Horseshoe on the Beaches of Rio. *The Mathematical Intelligencer*, 20(1):39–44, 1998.

[12] Steven H. Strogatz. *Nonlinear Dynamics and Chaos: With Applications to Physics, Biology, Chemistry, and Engineering*. CRC Press, 2018.

A Videos and Code

To view the k-lapse video, click on the following: https://vimeo.com/806196652.

To view the 3-dimensional bifurcation diagram, click on the following: https://vimeo.com/806201032.

To view the code to create 2- and 3-dimensional bifurcation diagrams on any interval of k_1 or k_2, see the following: https://github.com/AristotleTottle/Discrete-Predator-Prey/blob/9099183a54320dae10ed83978a6ef25945ad35ee/Bifurcation-Diagrams.R.

To view the raw code used during this research, see the following: https://github.com/AristotleTottle/Discrete-Predator-Prey/blob/9099183a54320dae10ed83978a6ef25945ad35ee/Raw-Code.R.